Thermal investigation of Three-Phase Induction Motors with an Integrated Open-Phase Fault Operation Using a Lumped Parameter Thermal Network (LPTN)

*

Mustapha Bouheraoua
Electrical engineering department,
Engineering Advanced Technology Laboratory(LATAGE), Mouloud Mammeri University of Tizi-Ouzou
Tizi-ouzou,Algeria
bouheraoua@hotmail.com

Mahdi Atig
Electrical engineering department,
Engineering Advanced Technology Laboratory(LATAGE), Mouloud Mammeri University of Tizi-Ouzou
Tizi-ouzou,Algeria
mahdiatig36@yahoo.fr

Rabah Khaldi
Electrical engineering department,
Engineering Advanced Technology Laboratory(LATAGE), Mouloud Mammeri University of Tizi-Ouzou
Tizi-ouzou,Algeria
khaldi_rabah@yahoo.fr

***Abstract*—The authors of this article present an analytical method based on a Lumped Parameter Thermal Network (LPTN) in order to model the effect of an open phase fault on the thermal behavior of an induction motor under steady state and transient thermal analysis. The heat transfer generated by the conduction and convection in induction motor are discussed. The results obtained by the model developed are validated by experimental tests. The tested machine is a standard three-phase, 4-pole, 2.2 kW, 380 V squirrel cage induction motor of Totally Enclosed Fan Cooled "TEFC" design manufactured in Algeria by Electro-Industries.**

Keywords — Conduction, Convection, Heating, Induction motor, Lumped parameter, Open phase.

I. INTRODUCTION

Induction motors (IMs) are the most robust and commonly used in industrial applications. However, to determine their different performances, their modeling is very important. Indeed, the modeling of these motors is needed in calculations of fault, voltage drop, control applications, transient analysis, etc. Induction motors (IMs), can be subject of several potential faults that affect safety, production and profitability of installations, such as the suppression of one or more stator phases of the motor, which requires special attention. However, in all three-phase induction machines, when one or more phases fail, the motor breaks down or at least cannot deliver any significant torque. In the presence of the open phase fault, these machines produce more heat on both stator and rotor winding. For that, during the last years, several investigations of induction motor behavior under an open-phase fault condition have been presented [1]-[5]. The presence of the open-phase fault in induction machines creates an unbalance in the temperature distribution of the motor, which requires an important need for accurate estimation of temperature, particularly in those hot spots where a risk of adverse thermal conditions increases. Indeed, to predict machine temperature, thermal models can be used to determine the maximum load ability during different operating conditions.

Due to the presence of a certain number of heat transfers inside the machine which will have to be identified and solved, the thermal study of these electrical machines is a very complex problem. Among these modes of heat transfer, we distinguish: conduction, natural and forced convection and radiation are all present. For thermal analysis, the two main approaches are numerical methods based on Finite Element Analysis (FEA) [5]-[9] and analytical Lumped Parameters Thermal Network (LPTN) [6]-[9], [11]-[16]. Commercial software packages as Matlab or Flux 2D using numerical methods based on Finite Element Analysis (FEA) or Computational Fluid Dynamics (CFD) can be used to simulate multidimensional problems with complex geometry. But their disadvantage lies in the computation time taken by the simulation of the encountered thermal problems in the machine, whether in two dimensional (2D) or especially in three dimensional problems (3D) and the parameters are often difficult to determine.

The problem of the long time simulation encountered by the finite element method mentioned above is solved thanks to the Lumped Parameter Thermal Network (LPTN). Often called the nodal method, it was initially developed for the electrical network analysis, and was quickly applied successfully to thermal systems. This method simplifies the heat transfer mechanism into a thermal network with lumped parameters. The main advantage of this method is the reduced computation time taken in solving the thermal problems of electrical machines and the ease in the introduction of the convection heat transfer coefficient in natural and forced cases. Previous thermal modeling studies were often focused on the machine in normal mode, in which the main heat sources are the constant maximum copper, iron and mechanical losses [9]-[16]. When the fault occurs in the machine, the current and flux density distribution changes their magnitudes according to the severity of the defect.

This paper is focused on the thermal behavior of an open phase fault of three phase squirrel cage induction motor for an industrial application. The machine is investigated during both healthy and faulty conditions. Thus, the main purpose of this paper is to study the influence of the open phase failure on the thermal behavior of an induction motor using an analytical method based on the Lumped Parameter Thermal Network (LPTN) validated by experimental study.

II. THERMAL MODEL FORMULATION

The (LPTN) approach is chosen to achieve a thermal model of a squirrel rotor cage induction motor with an open phase fault. This method is very old, but still remains an effective tool for solving the thermal problems encountered in electrical machines. Many researchers have used this method for solving heat transfer problems in electrical machines. Mellor's work remains a bibliographic reference in this field [11].This method exploiting the analogy between electric and thermal phenomena, the networks include resistances, capacities for the transient analysis, and current sources that represent the internal losses of the motor. More information and details about the method can be found in the references [11]. In order to model the thermal behavior of the machine with the defect, its geometry is discretized into basic elements in all three dimensions using cylindrical coordinates as shown in Fig.1 This results in the representation of the machine geometry of a set of small arc-segment elements with T-network illustration as shown in Fig.2,[17] The corresponding thermal resistance definition is given in (1) to (9), [17].

Because of the open phase fault, the heat transfer conditions in the three phase's stator winding are different [4], so it is necessary to represent each of them by a separate part (phase A, phase B and phase C). Due to the different losses generated in the different phases of the machine, the temperature distribution is different. In addition, each phase of the stator is considered divided into two parts: the slot winding and end-winding, since their thermal condition is also different.

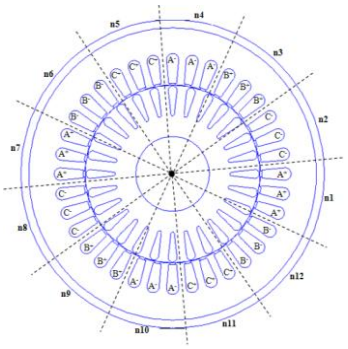

Fig. 1. Discretization of the machine geometry for thermal analysis with 12 arc-segment element

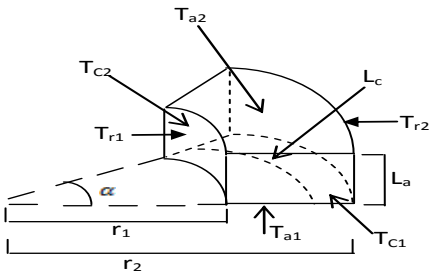

(a)

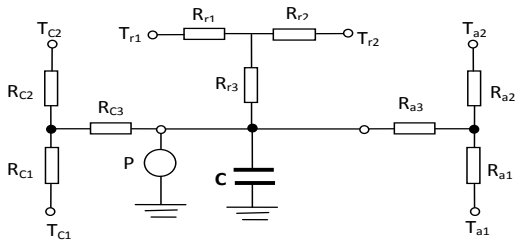

(b)

Fig 2. Geometric and T-network illustration of an arc-segment element [17].

$$R_{a1} = R_{a2} = \frac{180 l_a}{\alpha\pi\lambda_a(r_2^2 - r_1^2)} \quad (1)$$

$$R_{a3} = -\frac{60 l_a}{\alpha\pi\lambda_a(r_2^2 - r_1^2)} \quad (2)$$

$$L_c = \frac{\alpha}{360}\pi(r_1 - r_2) \quad (3)$$

$$R_{c1} = R_{c2} = \frac{L_c}{2\lambda_c L_a(r_2 - r_1)} \quad (4)$$

$$R_{c3} = -\frac{L_c}{6\lambda_c L_a(r_2 - r_1)} \quad (5)$$

$$R_{r1} = \frac{90}{\alpha\pi\lambda_r L_a}\left[\frac{2r_2^2 Ln\left(\frac{r_2}{r_1}\right)}{(r_2^2 - r_1^2)} - 1\right] \quad (6)$$

$$R_{r2} = \frac{90}{\alpha\pi\lambda_r L_a}\left[1 - \frac{2r_1^2 Ln\left(\frac{r_2}{r_1}\right)}{(r_2 - r_1)}\right] \quad (7)$$

$$R_{r3} = K\left[r_2^2 + r_1^2 - \frac{4r_2^2 r_1^2 Ln\left(\frac{r_2}{r_1}\right)}{(r_2^2 - r_1^2)}\right] \quad (8)$$

Where : $$K = \frac{-45}{\alpha\pi\lambda_r L_a(r_2^2 - r_1^2)} \quad (9)$$

According to this theory of the general arc-segment element, a whole Lumped Parameter Thermal Network (LPTN) under an open phase fault of the induction motor is developed and presented in Fig. 3. In this investigation, we note that the circumferential heat flow is not neglected. The circumferential heat flow has been considered only in the sta tor back iron and the corresponding thermal resistance definition is given by (4) and (5).

In order to evaluate with accuracy the magnitudes of the different resistances of the equivalent thermal network, it is necessary to know the different conductive heat transfer coefficient of the materials constituting the solid elements of the machine and especially calculate the different convective heat exchange coefficients h between the outer surface of the solid elements and the moving fluid inside the machine and the ambient. Indeed, the most important convective heat transfer coefficients to be evaluated are the convective heat transfer coefficient between the frame and the ambient, the convective heat transfer coefficient in the end-cap air and in the air-gap. This is due to the fact that in this last location, the main parts where the losses are generated are closest together. On the other hand, for the first, the temperature rise in the different components is very sensitive to the variation of the convective heat transfer coefficient of the ambient. In our case the areas where forced convection takes place is limited to the air-gap and around the end-winding and frame to ambient.

III. Parameter Estimation of the Equivalent Thermal Circuit

A. Convection Heat Transfer Coefficient in the Frame

Several researches have been done in the calculation of the heat transfer coefficient by convection between the frame and the ambient of electrical machines [15]-[19] and [20]. Since the modeling of the convective heat transfer from the machine surface to the ambient is more challenging, the most reliable way to calculate the convection heat transfer coefficient between the ambient and the external surface of the machine is to use the experimental tests on the machine. Within the literature, there exist many empirical correlations that are suited to the prediction of convection cooling from surface shapes typically seen in electrical machines. In this paper, to compute the heat transfer coefficient by convection between the frame and ambient it is enough to know the total losses P_{tot} generated inside the machine and to measure the temperature on its external surface and to fix the temperature of the environment. Indeed, the measured convection heat transfer coefficient between the frame and ambient is given by:

$$h = \frac{P_{tot}}{(\theta_f - \theta_a) A_{Fin}} \quad (10)$$

Where θ_f is the frame temperature (°C), θ_a is the ambient temperature (°C), $A_f = \left(A_1 + \eta A_f\right)$ is the frame effective area (m^2) with A_1 and A_{Fin} are the surface of frame casing which is directly in contact with the cooling air and surface of the fins respectively, η is the fin efficiency given in [15]-[19].

B. Convection Heat Transfer Coefficient in the Air-gap

It is known that the calculation of heat transfer coefficient by convection h_{gap} is very difficult Because of the rotation, the air flow in the air gap is turbulent and the heat transfer problem is more complicated. The *effective thermal conductivity coefficient* λ_{eff} is used and could be determined as [19].

$$\lambda_{eff} = 0.0019.\eta^{-2.9084}.R_e^{0.4614.Ln(3.33361\eta)} \quad (11)$$

Where $\eta = \frac{r_0}{r_i}$, r_i and r_0 are the stator inner diameter and rotor outer diameter (in meters), respectively. $R_e = \frac{r_0.\omega_e.d}{\upsilon}$, ω_e is the circular velocity of the rotor (in meters per second), d is the length of air gap (in meters), and ν is the cinematic viscosity of the air (in (m^2/s).

C. Heat Transfer between End-windings and End-cap Air

In the end-cap region, the end-winding space presents a particular problem because the flow conditions are not clearly defined since the air is turbulent in the enclosed space and there are no smooth or flat surfaces [18].
Due to the force convection in the region of the endcaps, the thermal resistance between winding and endcaps can be evaluated by the Convection thermal resistances for a given Surface as follow: $R = \frac{1}{h_C A}$; Again, the value of h_C is not simple to define. For totally enclosed machines, the value of h_C can be evaluated by (12) as a function of the air speed inside the motor endcaps [18] .

$$h_c = 6.22v \quad (12)$$

or by (13) to account for combined natural and forced convection [18] .

$$h = 41.4 + 6.22v \quad (13)$$

Other similar formulas are available in the bibliography and lead to the same results [14],[18]-[19].

In this study, the induction motor structure has been divided into 18 elementary components as reported in Table I.

Table I. Components of the Motor

Components	Nodes
Slot winding of phase A , B and C	1, 2 and 3
End winding of phase A , B and C	4,5 and 6
Stator yoke of phase A , B and C	7 ,8 and 9
Stator teeth of phase B , B and C	10 , 11 and 12
Rotor bars	13
Yoke	14
Air-gap	15
Shaft	17
Frame	18
End-cap air	16

For each component, a network such as that of Fig. 2 (b) is carried out. Then, the total network is obtained connecting together all the single component networks, and the number of each component in Table I refers to the corresponding node of the total network in Fig. 3. Once the total network obtained, the temperature rises in different elements under healthy and faulty operation are computed using Matlab/Simulink developed code, where the different heat capacities of different element of the machine are considered in the analysis of the transient operations. Table II gives some typical values for the thermal conductivities of solid materials and heat transfer coefficients used in the thermal investigation applied to the induction motor.

Table II. Thermal conductivities and film coefficients used in the thermal network.

Regions	Thermal conductivity $\lambda_x(x)/\lambda_y(y)$ (W/m·°C)	Film coefficient (W/m^2·°C)
Shaft steel	40	-
Lamination	1.98/45	-
Aluminum	204	-
Copper	386	-
Winding Insulation	0.15	-
Frame-ambient	-	123
Stator iron-frame	-	467
Air-gap	-	207
End-cap air	-	27

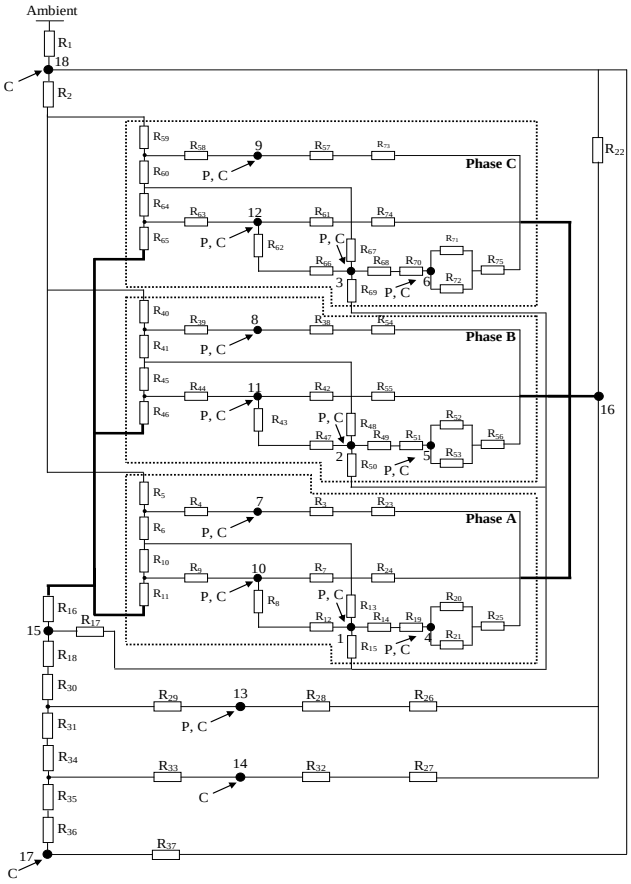

Fig. 3. A Lumped Parameter Thermal Network (LPTN) of a three phase induction motor under open phase fault.

IV. EXPERIMENTAL INVESTIGATION AND RESULTS ANALYSIS

In order to verify the proposed Lumped Parameter Thermal network (LPTN) model, a load testing platform is established. In this experimental procedure we will impose two different loads: 5.4 Nm and 9.1 Nm respectively. If the motor is fed from the load of 5.4 Nm, the r.ms value of motor current is about 2.1 A. But, when the phase A is opened, we noted that the new r.m.s stator currents I_1, I_2 and I_3 become 1.9 A, 3.35 A and 1.9 A, as shown in Fig. 5,[4]. The characteristic information on the tested induction motor is shown in Table III.

Table III. Component of the Motor

Parameters	Values
Rated power	2.2 kW
Enclosure type	TEFC
Frequency	50 Hz
Rated speed	1420 rpm
Rated voltage	380 V
Rated current	5.2 A
Rated Torque	15 Nm
Connection	Δ
Insulation class	F

In addition, the second test performed with a load of 9.1 Nm is the same as that of 5.4 Nm. The value of the current measured before the apparition of the defect is about 2.3 A, on the other hand the open-phase fault causes an imbalance of the currents in a similar manner with the above test which become 2.2 A, 4.3 A and 2.2 A.

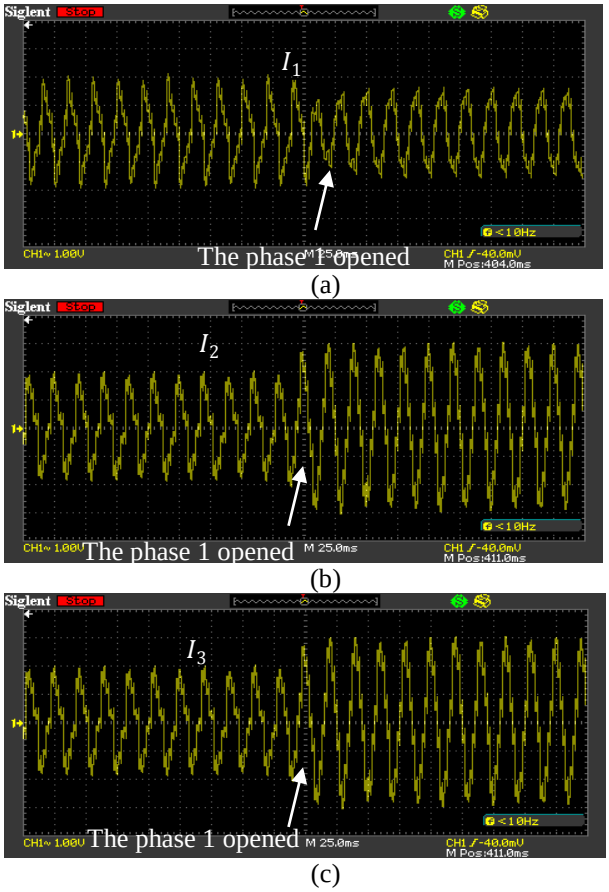

Fig. 5. The waveforms of currents (a) the current I_1 (b) the current I_2 and (c) the current I_3 with a load of 5.4 Nm for healthy and faulty operating conditions [4]

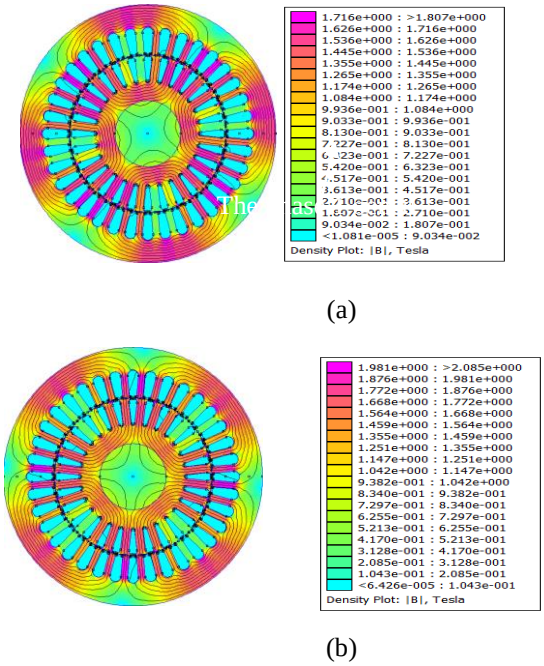

Fig. 6. Flux density distribution with a load of 5.4 Nm: (a) with healthy mode, (b) with the open phase fault

In this study, most power losses are calculated with the expressions of the balanced system. Indeed, the current obtained are used to calculate the losses in the stator

winding with and without the open phase fault. Thus, their waveforms are introduced into a finite element model to determine the maximum flux density of the motor, as shown in Fig.6. Then, this maximum value was introduced into the expression of the Steinmentz equation [21] used to calculate core losses per unit volume in magnetic materials.

The variation of B is not sinusoidal as is shown in Fig.7. A fast Fourier transform must be performed to separate the contribution of different frequency harmonics.

$$B_i(\theta) = \sum_{i=1}^{m} B_{i,n} cos\left(n\theta + \varphi_{i,n}\right) \qquad (14)$$

The power loss per volume unit for each harmonic is obtained for the K_{th} element from the classical expression.

$$P_{i,n} = K_h \cdot f_n \cdot B_{i,n}^{\beta} + K_e \cdot f_n^2 \cdot B_{i,n}^2 \qquad (15)$$

Where K_h is the hysteresis loss coefficient, f_n is the harmonic frequency, β is the hysteresis loss exponent, and K_e is the eddycurrent loss coefficient. These values are calculated from manufacturer data sheets. The iron loss density is then computed as the sum of the density contribution of the different harmonics by :

$$P_i = \sum P_{i,n} \qquad (16)$$

Iron losses are estimated and assigned separately for stator back iron and teeth to nodes (7, 8, 9) and (10, 11, 12) respectively. The contribution of these harmonics increases the size of these losses.

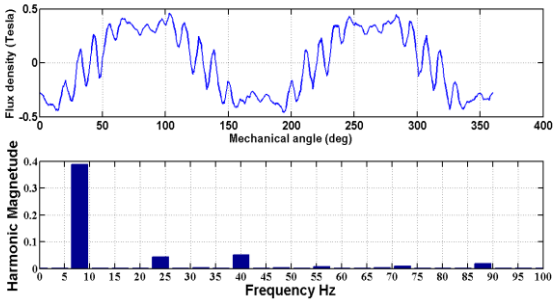

Fig. 7 Flux density distribution in stator Back iron and its FFT.

V. RESULTS AND DISCUSSION

In Fig.8 the measured temperatures have been compared with the simulation results for healthy and faulty operations in the frame, stator teeth, slot winding and end winding cooled side, for both transient and steady state conditions. In addition, a comparison between measured and simulated temperatures at steady state is illustrated in Table IV. Indeed, when the steady state is reached, we note that the worst discrepancy between the measured and the simulated temperatures is lower than 5.76 % for healthy operation and 7.65 % for faulty condition, which can be well accepted in this investigation. In addition, it can be seen that the open phase defect of the induction motor results in a temperature increase up to 50 % depending on the phase affected by the defect. According to the results obtained, we noted that the end winding cooled side reached a temperature of 75.1 °C with a load of 5.4 Nm and 119 °C with a load of 9.1 Nm, therefore with a rise of 43.9 °C for a difference of 3.7 Nm. Since the rated load of the induction motor is about 15 Nm with class F insulation, it is clear that the open phase at full load becomes impossible.

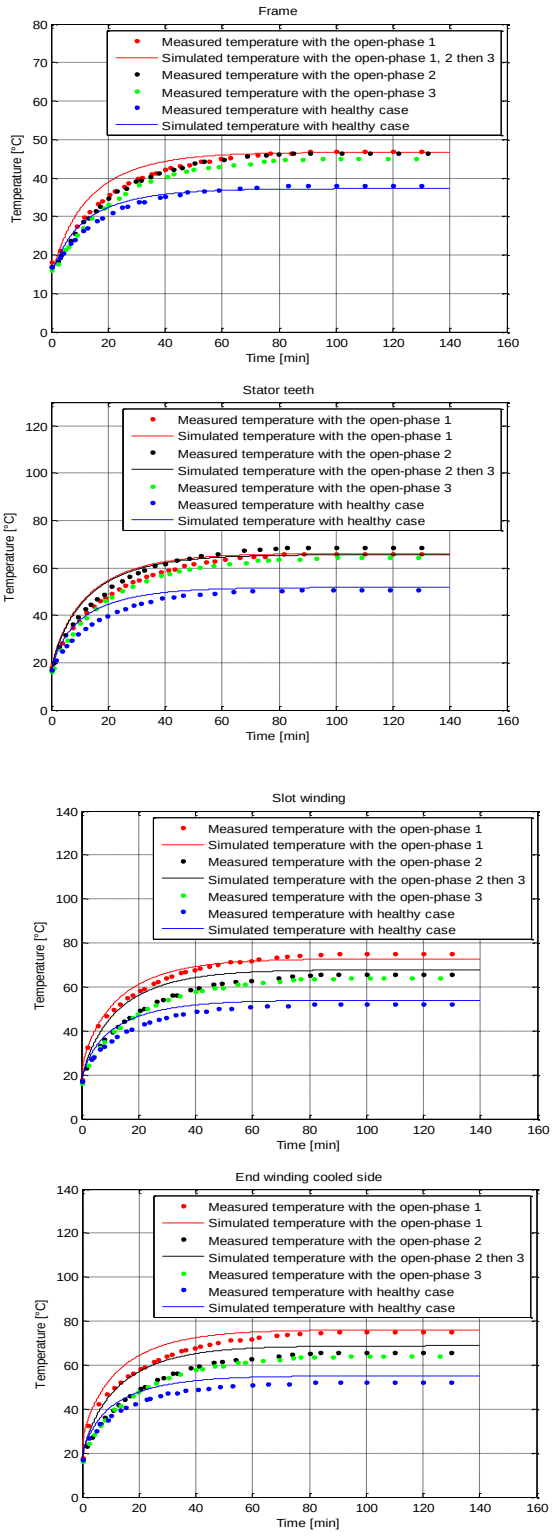

Fig. 8. Induction motor temperatures with a load of 5.4 Nm

Table IV. Steady state temperature comparison, with a load of 5.4 Nm

Modes	Tests	Frame	Stator teeth	Slot winding	End winding cooled side
Healthy mode	Measured	38.1	50.8	52.2	52.1
	Simulated	37.2	51.7	51	55.1
	Error %	2.36	1.77	2.87	5.75
Faulty mode with the open phase	Measured	46.9	65.9	75.1	75.1
	Simulated	46.6	66.1	72.8	76
	Error %	0.63	0.3	3	1.19
	Measured	46.5	68.5	65.6	65.6
	Simulated	46.6	65.5	67.8	68.7
	Error %	0.21	4.37	3.35	4.72
	Measured	45.1	64.4	64.2	64.2
	Simulated	46.6	65.5	67.8	68.7
	Error %	3.32	1.7	5.6	7

VI.CONCLUSION

The open phase fault of three phase induction motor has been studied in this paper. Focusing on the thermal behavior under fault operating conditions. The electromagnetic problem gives the image of the magnetic flux distribution in full defect for two different loads as well as the evolution of the current waveforms during faults. Experimental tests have been carried out in open circuit fault with which the developed LPTN model was validated. The tests are quite in agreement with the developed lumped parameter thermal model (LPTN).

Induction motors performances are strongly affected by the thermal states of their components. However, the development of the tool, giving real time information about the temperatures is a recommended solution. The lumped parameter method can be used to get an accurate value of temperature in different parts of the machine.
It is useful to note that the circuit of the Fig. 3 can also be used for a balanced three-phase supply with equal losses in each phase stator windings.

REFERENCES

[1] H. Guzman, M.J. Duran, B. Barrero, and S. Toral, "Speed control of five-phase induction motors with integrated open-phase fault operation using model-based predictive current control techniques," IEEE Transactions on Industrial Electronics, vol.61,no.9, pp.4474-4484,2014.

[2] A. Tani, M. Mengoni, L.Zarri, G.Serra and D. Casadej, "Control of multiphase induction motors with an odd number of phases under open-circuit phase faults IEEE Transactions on Power Electronics, vol. 27, no. 2, pp. 565-577, 2012.

[3] M.A. Fnaiech, F. Betin, G.A. Capolino and F. Fnaiech, "Fuzzy logic and sliding-mode controls applied to six-phase induction machine with open phases," IEEE, Transactions Electronics, vol. 57, no. 1, pp. 354-364, 2010.

[4] M. Atig, M. Bouheraoua, A.Fekik, "An experimental investigation of heating in induction motor under open phase fault," International Journal of Electrical and Computer Engineering (IJECE), vol. 8, no3, 2018.

[5] N. Bianchi, E. Fornasiero and S. Bolognani, "Thermal analysis of a five-phase motor under faulty operations," IEEE Transaction Industrial Applications, vol. 49, pp. 1531–1538, 2013.

[6] S. Mezani, S. Takorabet, and B. Laporte, "A combined electromagnetic and thermal analysis of inductions motors," IEEE Trans. Magnetics, Vol. 41, No. 5, pp. 360–372, *May 2005.*

[7] V. Madonna1, P. Giangrande,C. Gerada and M.Galea ,"Thermal analysis of fault-tolerant electrical machines for more electric aircrafet applications," J.Eng, vol.. 2018, Iss 13 pp. 461–467,January 2018.

[8] J. Fouladgar, and E. Chauveau, "''The Influence of the Harmonics on the Temperature of Electrical achines,"IEEE Trans. Magn.vol.41, no.5,pp.1644-1647,May 2005.

[9] M. Bouheraoua, N. Benamrouche, and A. Bousbaine, "A more refined Thermal Model for a totally Enclosed Fan-cooled Induction Motor," Electric Power Components and systems,Vol.40,Issue 2,2011.

[10] Q. Chen, Z. Zou, and B.Cao , "Lumped-Parameter Thermal Network Model and Experimental Research of Interior PMSM for Electric Vehicle," Electrical Machines and Systems, vol. 1, No.3,December 2017.

[11] P. H. Mellor, D. Roberts and D. R. Turner, "Lumped parameter thermal model for electrical machines of TEFC design," IEE Proceedings, Electric Power Applications, vol. 138, no. 5, pp. 205-218, 1991.

[12] A. Boglietti, D. Staton, D.Shanel, M.Mueller and C. Mejuto,"Evolution and modern approach for thermal analysis of electrical machines," IEEE Trans Industrial Electronics, vol.56, no.3,pp.871-882,2009.

[13] D.G. Nair, A. Rasilo, and A. Arkkio, "Sensitivity Analysis of Inverse Thermal Modeling to Determine Power Losses in Electrical Machines," IEEE Transactions on Magneticsl.vol.54,November 2018.

[14] A. Boglietti, A. Cavagnino, M. Popescu and D. Staton, "Thermal model and analysis of wound rotor induction machine ," IEEE Transactions on industry applications, vol.49, no 5, pp.2078-2085, 2013.

[15] A. Bousbaine, "An investigation into the thermal modelling of induction motors," Doctoral dissertation, University of Sheffield, 1993.

[16] C. Sciascera, P. Giangrande, and L. Papini, "Analytical thermal model for fast stator winding temperature prediction," IEEE Transactions on Industrial Electronics,vol.64, pp.6116–6126,Aug 2017.

[17] N. Simpson, R. Wrobel and P. H. Mellor, "A general arc-segment element for three-dimensional thermal modelling," IEEE Transactions on Magnetics, vol. 50, no 2, pp. 265-268, 2014.

[18] A. Boglietti, and A.Cavagnino, ",,"Analysis of the end winding cooling effects in TEFC Induction Motor''EEE Trans.Ind.App., vol.43,no.5,pp.124-1222,sep/Oct,2017.

[19] W. M. Rohsenow, J. P. Hartneh and E. N. Ganic, "Hand book of heat transfer fundamentals," Mc Graw-Hill, Inc. Second Edition, 1985.

[20] A. Valenzuela and J. A. Tapia, "Heat transfer and thermal design of finned frames for TEFC variable speed motors 'in *Proc. IEEE IECON*, Paris,France, Nov. 2006, pp. 4835–4840.

[21] C.P. Steinmetz, "On the law of hysteresis (originally published in 1892 '' *Proceedings of the IEEE*, vol. 72, no. 2, pp. 196–221,1984.

[22] P.S. Ghahfarokhi, A. Kallaste,A.Belahcene,T.Vaimann and A. Rassolkin, "Hybrid thermal model of a sychronous reluctance machine," Case studies in thermal Engineering,12 , pp. 381–389, september, 2018.